Recurrent interannual climate modes and teleconnection linking North America warm season precipitation anomalies to Asia summer monsoon variability

K. M. Lau, and H. Y. Weng*

Climate and Radiation Branch

NASA/Goddard Space Flight Center

Greenbelt, MD 20771

January 2001

(Submitted to J. Climate)

Corresponding author: K. M. Lau, NASA/Goddard Space Flight Center, Climate and Radiation Branch, Cod e913, Greenbelt, MD 209771

*Goddard Earth Science and Technology Center (GEST), University of Maryland at Baltimore County.

Abstract

In this paper, we present results showing that summertime precipitation anomalies over North America and East Asia may be linked via pan-Pacific teleconnection patterns, which are components of two dominant recurring global climate modes. The first mode (Mode-1) features an inverse relationship between rainfall anomaly over the US Midwest/central to the eastern/southeastern regions, coupled to a mid-tropospheric high-low pressure system over the northwest and southeast of the US, which regulates low level moisture transport from the Gulf of Mexico to the Midwest. The regional circulation pattern appears to be a part of a global climate mode spanning Eurasia, the North Pacific, North America and the Atlantic. This mode is associated with coherent fluctuations of jetstream variability over East Asia, and Eurasia, SST in the North Pacific and the North Atlantic. While Mode-1 is moderately correlated with ENSO, it appears to be distinct from it, with strong influences from mid-latitude or possibly from higher latitude processes. Results show that Mode-1 not only has an outstanding contribution to the great flood of 1993, it has large contribution to the US precipitation anomalies in other years. Also noted is an apparent increase in influence of Mode-1 on US summertime precipitation in the last two decades since 1977.

The second mode (Mode-2) is associated with continental scale rainfall anomaly over the US characteristic of the severe drought 1988. Similar patterns of precipitation

extremes, albeit with less intensity are found to occur in other years. Mode-2 depicts a large scale mid-tropospheric high over much of the US continent, which appears to be a part of a wavetrain signal emanating from the subtropical western Pacific, across the North Pacific to North America. Regression analysis suggests that Mode-2 is dynamically consistent with Rossby wave dispersion excited from fluctuations of heat sources and sinks the Indo-Pacific monsoon. Results from analysese keyed to the regional fluctuations of the Asian monsoon confirm the presence of the teleconnection signals linking precipitation anomalies over North America and East Asia.

Overall, our results suggest that summertime precipitation anomalies in the US may be linked by teleconnections to Asian monsoon variability, via jetstream variability and tropical heating embedded in global recurring climate modes. We argue that these global modes may be important in better understanding of how the large-scale circulation may provide the requisite pre-conditioning to facilitate regional land-atmosphere interaction, leading to summertime severe droughts and floods over the North America and East Asia.

1. Introduction

Severe droughts and floods caused by summertime precipitation extremes are among the most costly natural disasters affecting the climate of North America. Yet compared to wintertime severe weather, the mechanisms of summertime precipitation anomalies are much less understood and the prospect for long-term prediction is not as promising (Mo and Kalnay 1991). Causes of summertime precipitation anomalies have been attributed to a large number of factors including tropical and extratropical sea surface temperature (SST), large-scale atmospheric circulation, land surface processes, and land-atmosphere feedback processes. Several earlier studies (Trenberth et al 1988, Trenberth and Branstator 1992, Palmer and Brankovic 1989) suggested the possible influence of La Niña on the summertime droughts of 1988. Others have suggested the importance of transient forcings (Chen and Newman 1998). Moreover, GCM simulation using only SST anomalies without proper initial conditions, were largely unsuccessful in reproducing the 1988 drought (Mo et al 1991). Studies of the great flood over the US Midwest in 1993 led many authors to conclude that remote forcings including diabatic heating over the western Pacific, and atmospheric transient forcings coupled with land surface processes may be contributing factors (Trenberth and Guillemot 1995, Ting and Wang 1997, Mo et al 1997, Liu et al. 1998, Bosilovich and Sun 1999, and Higgins et al. 1999).

Recent studies have demonstrated that the potential predictability of US precipitation (both winter and summer) is dependent of the interplay of multi-scale processes ranging from intraseasonal, interannual, decadal to secular changes in the climate system (Higgins et al 2000, Mo 2000, and Livezey and Smith 1998). Up to now, most of the observational and theoretical studies of U.S. drought and flood have mainly focused on case studies for 1988 and 1993, deemed as episodic events. These studies also tend to emphasize the impacts of known natural climate cycles, e.g. the Madden-Julian Oscillation, ENSO, the Pacific Decadal Oscillations, and the North Atlantic Oscillations, on US climate variability. Yet, there have not been much studies of the root causes of summertime precipitation variability over the US, especially with regard to the possibility that the summertime climate extremes may stem from regional amplification of recurring global climate modes, which may be distinct from those associated with the aforementioned natural climate cycles.

To identify possible recurring global modes affecting summertime regional precipitation over the US, the source regions for energy and water have to be considered. During boreal summer, the most dominant sources of energy and moisture that drive the atmospheric general circulation are found in the Asian monsoon region. Previous investigators have noted that during boreal summer, convective heating over the subtropical western Pacific near the Philippines can excite a wavetrain pattern that spans the northern rim of the Pacific Ocean and North American (Nitta 1987, Huang 1985). Lau

and Peng (1992) and Lau (1992) showed that a wavetrain-like teleconnection pattern may stem from marginally unstable normal modes of the summertime large-scale monsoon circulation. Chen (1993) pointed out the importance of summertime stationary eddies and their linkages to tropical SST and the Asian monsoon variability. A number of authors (e.g. Lau et al 2000, Wang et al 2001, Li and Zhang 1999 and others) noted strong trans-Pacific wave signals emanating from the South China Sea, through the Aleutians to North America during period of enhanced East Asian monsoon activities. More recently, Lau and Weng (2000) reported wavetrain patterns associated with US summertime precipitation that suggest apparent sources in the Asian monsoon. However, the relationship of these wavetrains to precipitation anomalies over the US and over Asia continents has not been firmly established. In this paper, we expand on the above studies to explore the root causes of summertime precipitation anomalies over the US continent, with emphases on the teleconnections linking the Asian monsoon and North America precipitation and circulation anomalies.

2. Data and Analysis Procedure

In this study, we use monthly mean rainfall of 102 divisions over the continental United States from the National Center for Environmental Predictions (NCEP), monthly mean wind and geopotential height fields from the NCAR/NCEP reanalysis (Kalnay et al. 1996), monthly sea surface temperature (SST) from the Hadley Centre for Climate Prediction Research, the United Kingdom. The seasonal mean for the summer is

defined as the average over June-July-August (JJA), for all the field, except for rainfall where the 3-month total is used. The analysis period is 1955-1998. All the anomalies are calculated as departures from the temporal mean for the 1961-90 base period. Since both interannual and longer time variability are expected to contribute differently to US rainfall variability they should be studied separately. Accordingly, we decompose the seasonal data into Fourier harmonics with the interannual component defined by harmonics with periods from 2-8 years, and interdecadal components with periods longer than 8 years, using a subroutine provided by J. Alquist, Florida State University. In this paper, we only deal with the interannual component. We use Empirical Orthogonal Function (EOF) to identify the dominant modes of US summertime rainfall and to estimate the effective number of spatial degrees of freedom of the rainfall field (Bretherton et al 1999). To explore the influence on rainfall variability due to a specific forcing function i.e., SST or large scale circulation, we use the method of Singular Value Decomposition (SVD) to identify the dominant rainfall patterns that are maximally correlated with the chosen forcing function (Wallace et al. 1992).

In the present work, we use SVD analysis with the full awareness of its inherent caveats, in particular the possibility that the selected modes may be non-physical (Cherry 1997, Newman and Sardesmukh 1995, Lau and Weng 2001). To ensure reliability, the SVD computations have been carried out with the rainfall anomalies coupled to different co-varying fields. In addition, the SVD results have been tested against EOF analysis and

compared to reconstruction of the observed rainfall anomalies, and to simple one-point correlation and regression patterns of various dynamical variables to reassure physical consistency and the robustness.

3. Preliminary observations

In this section, we highlight basic features for the 1993 flood and the 1988 drought to provide the background and motivation for the main analyses in subsequent sections.

a. Rainfall and Circulation anomalies in 1993 and 1988

Figure 1 shows the seasonal mean anomalies of rainfall over continental US and of the global circulation in the summer of 1993. Notably, the rainfall anomaly is not only restricted to the Midwest region, but appears in the form of a dipole with positive anomalies over the Midwest and central northern states, and negative anomalies over the eastern and southeastern states (Fig. 1a, left panel). The associated global 500 hPa geopotential and 850 hPa wind patterns (Fig. 1b, left panel) feature a zonally oriented wavetrain along 30-50°N, stretching from the northeastern Asia/Japan region, across the North Pacific, to North America and the North Atlantic. A second wave signal appears over the land region of northwestern Europe, with possible connection to the Atlantic anomalies across the polar region. Over North America, the most prominent feature is a mid-tropospheric cyclone-anticyclone couplet linking the northwestern and the southeastern states, with enhanced low level flow from the Gulf of Mexico to the Midwest region. This circulation pattern is consistent with the enhancement of the low-

level jet over the great plains during the summer of 1993, as reported in many previous studies. In the tropics, the wind anomalies are generally weak. The velocity potential and divergent wind anomalies (Fig. 1c, left panel) suggest anomalous rising motion over the tropical eastern Pacific and sinking motion over the maritime continent and the Indian Ocean. These circulation features are consistent with the moderate warming in the tropical eastern Pacific during the summer of 1993.

During severe drought of 1988, the rainfall pattern shows a widespread negative anomaly over the entire US continent, except the southwest region (Fig.1a, right panel). Again, the center of the rainfall anomaly is found over the Midwest and the central US. The 500 hPa geopotential and 850 hPa wind anomalies show enhanced tropical and extratropical activities (Fig.1b, right panel). An apparent wavetrain signal emanates from the South China Sea /Philippines region, across Kamchaka and the Aleutians, to North America and the Atlantic regions. A second wavetrain can also be seen over the Eurasian continent which appears to merge with the aforementioned wavetrain over the Pacific region. Over North America, the large scale circulation is dominated by a positive 500 hPa height anomaly, with the Midwest regions under the influence of northerly flow from Canada. Compared to 1993, the tropical wind anomalies in 1988 are stronger, as evident in the 200 hPa geopotential anomaly (Fig 1c, right panel), which shows large negative divergence (subsidence) over the central equatorial Pacific, and positive divergence (ascent) over the Indian Ocean. The divergent circulation anomaly

can be identified with the eastward shift of the Walker Circulation during the La Niña of 1988. Overall, the observations suggest that the circulation anomalies affecting the US region may be a part of global circulation pattern with possible sources in the western Pacific and the Eurasian region.

b. One-point correlation

Although the rainfall and circulation anomaly patterns for 1993 and 1988 are quite distinct, the central states and Midwest region of the US appear to be a focal point of some dominant global teleconnection patterns. To explore this, a one-point correlation map of the global 500 hPa height and SST fields, keyed to the JJA mean rainfall anomalies averaged over the region [35-47° N, 100-85°W], has been computed. It is quite clear from Fig. 2a that the rainfall anomalies over the US Midwest region are connected to a regional circulation pattern which is a component of a global wavetrain pattern, with linkages to the western Pacific/Maritime continent, and Eurasia. The correlation pattern remains essentially the same even after the years 1993, and 1988 are removed from the analysis (not shown), providing evidence that the two events stem from intrinsic modes that are operative throughout the data period.

The aforementioned circulation anomalies are related to coherent variations of sea surface temperature over the Pacific and Atlantic oceans as evident in the global SST correlation map based on the same reference rainfall anomalies as shown in Fig. 2b. The largest SST loadings are found over the extratropical North Pacific, with large

negative anomalies in the Sea of Japan and the central North Pacific, and positive anomalies along the west coast of North America. Above normal SST is found in the vicinity of the maritime continent, and the Indian Ocean. The SST anomalies in the Sea of Japan and the oceanic regions surrounding the maritime continent constitute the characteristic dipole pattern associated with the interannual variations of East Asian monsoon (Lau et al 2000, and Weng et al 1999). As evident in the lack of a strong SST signal in the equatorial central and eastern Pacific, the SST pattern shown in Fig. 3b is *not* fundamental to ENSO, even though it may have non-zero projection on the characteristic JJA SST pattern for ENSO (Lau and Wu 1999, and Lau et al 2000). The extratropical SST pattern appears to be consistent with atmospheric forcing as suggested by Lau and Nath (1996).

3. Results

a. EOF rainfall analysis

The first EOF explains 20% of the rainfall variance, depicting a dipole rainfall patterns with centers over the Midwest, and the east and southeastern states (Fig 3a). This pattern is similar to that occurred during 1993 (see Fig. 1a). The second EOF mode shows a continental scale rainfall anomaly centered over the Midwest and central states, with anomalies of the opposite sign over the southwest and the northeast (Fig.3b), capturing much of the rainfall anomalies in the summer of 1998. The principal components (PC) in Figs. 3c and 3d show that both EOF1 and EOF2 projects strongly on

the 1993 Midwest flood, and that EOF2 alone contribute to the drought event of 1998. It is noted from the two PCs that in the decades after the late 1970's, there is an increase in the amplitude of the fluctuations. We find that N (= 15) EOF modes are needed to account for 90% of the total rainfall variance, and according to the rule-of-thumb of Bretherton et al (1999), we estimate the effective number of spatial degrees of freedom in the rainfall field to be N –1 (=14). The degree of freedom will be used to estimate the confidence level in the subsequent correlation computations.

b. SVD Analysis

1) RAINFALL AND 500 HPA HEIGHT FIELD

As stated in Section 2, SVD analysis is carried out to facilitate the physical interpretation of the dominant rainfall patterns, with respect to the large-scale forcings. Figure 4 shows the spatial and temporal pattern of the first SVD modes (Mode-1) between US rainfall and 500 hPa height field in the domains shown. Mode-1 explains 32% of the squared covariance between the two fields, and features a rainfall pattern that is broadly similar to that for EOF1, with a dipole structure linking rainfall anomalies in the Midwest and northern central states to anomalies of the opposite sign in the eastern and southeastern states. More interesting, the Mode-1 rainfall pattern appears to be associated with a 500 hPa cyclone-anticyclone couplet over the northwest and southeast North America, connecting to an extensive zonally elongated height anomaly, which spans the North Pacific, reaching Japan and the northeastern China. The zonally banded

structure over the East Asian sector (110° -150° E) can be identified with a characteristic pattern arising from the fluctuation of the East Asian jetstream (Lau et al. 2000). The PC (Fig.4c) shows that Mode-1 has the largest positive projection (>2 standard deviation) in 1993, but has negligible contribution in 1988. Large projections (> one standard deviation) are also evident in other years, notably 1994, 1989, 1968, 1967, 1961 and 1955, suggesting that Mode-1 may represent recurring climate modes.

The second SVD mode (Mode 2) in Fig. 5a depicts a widespread, continental scale rainfall pattern with center over the central U.S. with anomalies of the opposite sign in the northwest and the southwest similar to that shown in EOF2. Associated with the rainfall pattern is a pronounced wavetrain spanning the entire North Pacific, which appears to emanate from the East Asia/Japan region (Fig.5b), similar to the correlation map shown in Fig. 2a. In Mode-2, much of the continental North America is dominated by a pronounced high centered to the northwest of the Great Lakes, while the northwest and Alaska are controlled by a prominent low. The PCs (Fig. 5c) show large amplitude swings, producing rainfall deficits over the central US for recent decades in 1983, 1988 and 1991, while rainfall excesses are noted in 1982, 1992, and 1998. During 1993, Mode-1 dominates, but Mode-2 contributes significantly, reinforcing to yield excessive rainfall over the Midwest region. During 1988, Mode-2 is the dominant contributor to the continental scale rainfall deficit. As we shall show later, the causes of the observed rainfall anomalies for all years depend largely on the interplay of the physical

mechanisms underlying Mode-1 and Mode-2. Higher modes contribute to sub-regional scale variability, which may be important for individual years (see Section 3d for further discussion).

2) RAINFALL AND SST

To reassure the physical consistency of the aforementioned rainfall and teleconnection patterns, we have computed the SVD patterns for JJA rainfall and SST over the domain shown in Fig. 6. Again, the Midwest-East Coast rainfall dipole emerges as the dominant mode (Fig. 6a). The similarity of the SST-based and the height-based rainfall patterns leaves little ambiguity that they are intrinsic modes of the system. Although the Mode-1 SST pattern has some resemblance to El Niño SST anomaly in the tropics, it has distinct features that are not typical of El Niño. The most prominent feature is a large pool of zonally oriented cold water in the north Pacific along 40° N, which coincides with the 500 hPa anomaly associated with Mode-1 (see Fig. 4b). The extratropical cold tongue over the western Pacific coupled with the warm water to the south over the East China Sea and oceanic regions surrounding the maritime continent provide a region of increased meridional SST gradient off the coast of East Asia. This increased gradient is an important factor in governing the fluctuation of the summertime East Asian jetstream and the west Pacific subtropical high (Lau et al 2000). The PCs shown in Fig. 6c, are highly correlated with those shown in Fig. 4c. A

regression of the PC of SVD1 of US rainfall and 500 hPa against SST (not shown) can reproduce the same SST features shown in Fig. 6b.

Similarly, the continental scale rainfall variability of Mode-2 is captured by SVD2 of the coupled rainfall-SST analysis (Fig. 7a). The SST pattern in Fig. 7b shows that associated with a below-normal rainfall condition over the central US, the strongest SST signal is found in the extratropics with warm anomaly in the subtropical central Pacific, cold anomalies in the North Pacific, south of the Kamchatka Peninsular, and the Gulf of Alaska and off the west coast of North America. Cold water is also found over in the Atlantic adjacent to the east coast of North America. The cold SST surrounding the North America continent and the warmer land temperature associated with reduced rainfall, may have provided the anchoring for the portion of the wavetrain found over North America associated with Mode-2 (see Fig. 5b). The Mode-2 SST pattern is quite similar to the one-point correlation SST map, based on area-averaged Midwest rainfall, as shown in Fig. 2b.

3) GLOBAL TELECONNECTIONS

In this section, we further explore the physical underpinnings of the teleconnection patterns associated with Mode-1 and Mode-2. Regression of the Mode-1 PC of US rainfall-SST against the global 500 hPa geopotential and 850 hPa wind and 200 hPa velocity potential have been computed. For Mode-1 (Fig.8a), a pan-Pacific jetstream pattern emerges as the most distinct feature in the 500 hPa field. In addition, wave

signals are noted over western Europe possibly connecting with the Atlantic region via the polar regions, similar to those shown in Fig. 2a. The 850 hPa wind anomaly is consistent with the 500 height anomaly, indicating quasi-geostrophic flow, with deep vertical structure at least up to the mid-troposphere. Over the US continent, the enhanced low level flow from the Gulf region into the US Midwest, is quite obvious. Figure 8a strongly suggests that the regional circulation over the US is a part of a global pattern associated with extratropical stationary waves and jetstream variability along latitude belts between 30°-60° N. Mode-1 also features strong low-level wind signal in the equatorial central Pacific and the maritime continent. The 200hPa velocity potential regression (Fig.8b) suggests that Mode-1 may be related to the fluctuation of the Walker and local Hadley cells, driven by heat sources and sinks in the western Pacific/maritime continent and the Mexican monsoons. The divergent circulation associated with these overturning cells may cause the midlatitude jetstream to accelerate or decelerate, effectively providing a source of vorticity for downstream wave development (Sardesmuckh and Hoskins 1988, and Lau and Peng 1992). The association of Mode-1 with the Walker circulation, however may only be partial, because the jetstream may also be influenced by polar processes, which are not well represented by the velocity potential.

The Mode-2 regression pattern suggests a global Rossby wave pattern, with an apparent heat source in the equatorial Indo-Pacific region (Fig. 8c). The low-level

anticyclonic feature to the northeast of the Philippines is a characteristic feature of the Asian summer monsoon which regulates the rainfall of East Asia (Wang et al 2001, Lau et al 2000, Lau and Wu 2001). The apparent heat source is evidence in the divergent center in the Indian Ocean in Fig. 8d. Elsewhere, the upper level divergent and convergent patterns are consistent with the wavetrain signal shown in Fig. 8c. The overall velocity potential pattern suggests that in addition to heat sources of the Indo-Pacific monsoon, those associated with the Mexican monsoon may be important in forcing the Mode-2 response.

c. Rainfall reconstruction

To determine the contributions of various SVD modes, and by inference their underlying physical mechanisms, to specific occurrence of precipitation extremes, Fig. 9 shows the mode-by-mode reconstruction of rainfall anomaly from the SVD modes for the great summer flood of 1993. It can be seen that Mode-1 alone (Fig. 9a) capture the Midwest-east coast rainfall dipole and almost all the observed anomaly features (Fig. 9f). The correlation of SVD1 and the observation is 0.83. Addition of other modes does not alter much the correlation, but increases the explained rainfall variance. Hence for the 1993 event, Mode-1 and by inference its underlying dynamics, i.e., East Asian jetstream variability, is important in contributing to the observed rainfall anomaly pattern.

The rainfall reconstruction shows a somewhat more complex situation for 1998 (Fig. 10). Here, the contribution of Mode-1 is almost negligible, with a spatial

correlation less than 0.1. The addition of Mode-2 increases the correlation to 0.4. Higher order modes are required to increase the explained variance and to fine-tune the locations and the magnitude of the anomalies. However, re-construction even up to the first five modes, yields a correlation that is lower (= 0.55) compared to the 1993 case, suggesting some higher order processes not included in the global modes may be important for the 1988 drought. The importance of Mode-2 in 1988 suggests that wavetrain excited from convection over the Indo-Pacific monsoon region may be, at least partially important, in forcing the large scale circulation anomalies, and in pre-conditioning the 1988 US drought. However, the East Asian jetstream variability (Mode-1) appears to have little impact in 1988.

Figure 11 shows the cumulative anomaly correlation (CAC) for the first five modes for all years. The dominant contribution of Mode-1 to the observed rainfall anomaly is in 1993 is obvious (> 99% confidence level). Mode-1 also contribute significantly (>95% confidence level) in other years, i.e., 1998, 1994, 1990, 1989, 1987, 1971 and 1955. By comparison, strong Mode-2 events (greater than or close to 95% confidence level) occur with less frequency, notably in 1995, 1988, 1976 and 1958. The inclusion of higher order mode generally increases the CAC. Notice that there appears to be an increase in the CAC for the first five modes, and increasing frequency of strong Mode-1 contribution after the late 1970s. Table 1 summarizes the statistics of the relative importance of Mode-1 and Mode-2 in contribution to US summertime precipitation anomalies. The

combination of Mode-1 and Mode-2 produces a CAC that is equal to or exceeds the 99% confidence level for 23 out of the past 44 years. Noteworthy is the increasing contribution by Mode-1 in the decades after 1977, possibly related to the secular shift in the Walker Circulation (Kumar et al 2000, Krishnamurthy and Goswami 2000). The increasing dominance of Mode-1 on US summertime precipitation anomalies may also be related to the shift towards a warmer tropical SST and a corresponding shift in the global circulation before and after the 1976-77 as noted in a number of previous studies (Lau and Weng 1999, and Graham 1994).

Similarly, the CAC can be computed using the SST-PCs instead of the rainfall-PCs (Fig.11b). The CAC based on SST-PC provides an estimate of the maximal rainfall information content that can be derived from "perfect" knowledge of the SST field. As expected, there is a general reduction in the CAC based on SST compared to those based on rainfall, because the coupling between SST and rainfall is far from perfect. However, for the "tall poles", the reduction in CAC contribution by Mode-1 and Mode-2 is only minimal. Most of the reduction occurring when the CAC is already not very high. This suggests that SST anomalies are more likely to make an impact on the US summertime rainfall anomalies only in conjunction with the occurrence of Mode-1 and/or Mode-2.

4. Further discussions

In this section, we examine the converse of the teleconnection linkages suggested by the results of the previous sections, i.e., teleconnection arising from Asian monsoon

anomalies. Weng, Lau and Xue (1999) and Lau and Weng (2001) (hereafter referred to as WLX and WL) have identified the intrinsic modes of co-variability of China rainfall and global SST using SVD and regression analyses. However, their analyses included both interannual and longer-term variations. Here, we have re-computed the SVD modes of China rainfall and SST for interannual component only (< 8 years) as for the US precipitation to facilitate the comparison between the two analyses.

a. Teleconnection patterns associated with Asian monsoon variability

Three intrinsic modes, which are nearly identical to those reported in WLX and WL have been identified. Briefly, the first is the ENSO-monsoon mode, which portrays the direct impact of ENSO on the Asian monsoon, with a teleconnection pattern that describes the eastward shift of the Walker circulation and the global monsoon circulation associated with ENSO (not shown). The second and third are regional modes associated with the fluctuation of the East Asian monsoon and regional SST variability. The readers are referred to WLX and WL for more detailed discussion of these intrinsic modes. Here, only features directly relevant to teleconnection patterns of Mode-1 and Mode-2 will be discussed.

The second China rainfall-SST mode (SVD2) in Fig. 12a shows a zonally oriented rainfall band over the Yangtze River region along 30° N, with anomaly of the opposite sign in southern China . The co-varying SST pattern for SVD2 (Fig.12b) depicts a meridional SST dipole off the coast of East Asia, as noted in the SST pattern for Mode-1

(see Fig. 6b). The third SVD mode (fig.12c) shows a rainfall pattern with the center of positive anomalies shifted northward to northern China near the Huai River, with reduced rainfall south of the Yangtze River. This rainfall pattern is associated with extratropical wavelike SST anomalies (Fig.12d) which resemble those shown in Fig. 6b. The regressions of the PCs of the aforementioned regional monsoon modes against the 500 hPa geopotential and 850 hPa wind field are shown in Fig. 13.

The SVD2 teleconnection (Fig. 13a) is similar to that of Mode-1, and implies that a positive rainfall over the Yangtze River region may be linked to enhanced rainfall over US Midwest. The relationship is physically plausibly because the *Mei-yu* rainfall over the Yangtze River is strongly controlled by the fluctuation of the East Asian jetstream associated with the variations of the local Hadley circulation (Lau et al 2000). As we have shown in previous sections, the precipitation anomaly over the US Midwest is governed by the cyclone-anticyclone couplet that regulates the amount of moist Gulf air reaching the Midwest region. Our results indicate that these two widely separated regional features could be linked by jetstream variability as part of a global recurring climate mode.

Similarly, the SVD3 teleconnection (Fig. 13b) suggests the presence of a symmetric heat source in the Indo-Pacific region with Rossby wave patterns, which are governed by wave energy dispersion on the sphere (Nitta 1987). The waveguide set up by the East Asian jet will be important in determining the exact path along which the Rossby

wavetrain propagates. Alternatively, the wavetrain may also be a manifestation of instability of the summertime monsoon circulation (Lau and Peng 1992). The heat source is related to, among others, the east-west shift of the position of the subtropical high, resulting in generation of a low level anticyclone off the northeast of the Philippines, which causes the East Asian *Mei-yu* rain belt to shift north of the Yangtze River.

b. Asian monsoon indices

In this subsection, we offer additional evidence pointing to the presence of teleconnection signals linking the Asian and the North American continent in boreal summer. In a recent paper, Lau et al (2000) classified the Asian summer monsoon into a South Asia and a Southeast-East Asian component, distinguishing the former as the "classical monsoon" and the latter as the "hybrid monsoon" having strong tropical as well as extratropical dynamical characteristics. It was pointed out that the East Asian monsoon is an effective "communicator" of monsoon effects to other global circulation systems, because of the influence of the East Asian jetstream. They also proposed a regional East Asian monsoon index (EAM), which is a measure of the meridional shift in the position of the East Asian jet, associated with rainfall variability over regions covering central and North China, Korea and Japan. Similarly, Wang and Fan (1999) and Wang et al (2000) proposed an index for the Western North Pacific Monsoon (WNPM), focusing on variability of convection over the western Pacific near the

Philippines. These two indices are not entirely independent but may be considered as basic measures of the distinct regional components of the Asia monsoon.

Fig. 14 shows the regression of 850 hPa wind and rainfall anomalies over China and US against EAM and WNPM indices respectively. The EAM regression shows a wavetrain pattern linking summertime rainfall anomalies over East Asia and North America, connected by a strong low level cyclonic flow over the central North Pacific. This pattern appears to be the counterpart of Mode-1, with strong signals over East Asia, somewhat weaker but discernible signal over the US. Over East Asia, the rainfall has a dipole pattern, with above normal rainfall over central China and below normal rainfall over northeastern China. Over the U. S., the Mode-1 rainfall dipole is very clear. The regressed rainfall magnitude (order of 15-20 mm) is comparable to that of the observed. Since the EAM is essentially an index derived from the fluctuation of the East Asian jetstream, the present results further underscore the importance of the East Asian jetstream in effecting the Mode-1 teleconnection.

Similarly, the WNPM regression indicates a strong wind signal over the equatorial Indo-Pacific region (Fig.14b). Clearly the WNPM regression captures the variability of the Asian monsoon in the equatorial region, as evidence in the strong easterly wind from the western Pacific across Indochina and India. The signatures of the West Pacific anticyclone, and zonally banded wind structure along the coast of East Asia characteristic of the East Asian monsoon are also very clear (Lau et al 2000). The rainfall pattern

suggests a northward shift of the rainfall into northern China, and an expansion of the dry region to the eastern and central U.S, signaling a continental drought. The wind and rainfall patterns associated with WNPMI suggest a mixture of Mode-1 and Mode-2 responses.

5. Conclusions

In this paper, we have presented evidence that summertime precipitation anomalies in the North American continent and in the Asian monsoon regions may be linked by teleconnection patterns which are components of recurring global climate modes in boreal summer.

Two dominant climate modes governing precipitation anomalies over the U. S. have been identified using EOF, SVD and regression analyses. The first mode (Mode-1) features an inverse relationship between rainfall anomaly over the Midwest/central states, and the eastern/southeastern regions, and an atmospheric teleconnection pattern that spans Eurasia, the North Pacific, North America and the Atlantic. The pattern consists of extensive, zonally oriented 500 hPa height anomalies over the North Pacific, a high-low mid-tropospheric geopotential couplet over the northwest and southeast of the US continent, and a low level meridional flow over the Great Plains, which regulates moisture transport from Gulf of Mexico to the Midwest and Central States. Mode-1 is found to have outstanding contribution to the great flood of the Midwest in 1993, and also have large contributions in other years, notably 1998. While the associated

circulation and SST patterns have non-zero correlation with El Niño, Mode-1 appears to depict a distinct circulation system arising from fluctuation of the East Asian jetstream, and variations of SST in the North Pacific. Compared to the previous bi-decade (before 1977), the last bi-decade (after 1977), Mode-1 appears to be increasingly important in contributing to summertime rainfall anomaly over the US.

Mode-2 portrays a rainfall deficit (excess) over the central US and the east, with opposite sign rainfall in the west, coupled to a large scale mid-tropospheric high (low) over the central and eastern US continent. This mode is associated with a pan-Pacific wavetrain connecting the subtropical western Pacific, via the Aleutians to northern North America. Mode-2 is consistent with Rossby wave dispersion derived from fluctuation of anomalous heat sources and sinks in the western Pacific and Indian Ocean, as well as marginally unstable summertime basic state found in previous studies (Nitta 1987, Lau and Peng 1992). Results suggest that tropical heating in the western Pacific and wavetrain dynamics (via Mode-2), may be important contributing factors to the severe continental scale drought over the US continent in 1988, and to similar but less severe large scale rainfall deficit over the central US in other years.

Complementary to teleconnection pattern based on US rainfall, we find that fluctuations of the East Asian monsoon rainfall based on mode decomposition as well as monsoon indices can give rise to teleconnection patterns resembling Mode-1 and Mode-2 derived from US rainfall anomalies. Overall, our results suggest that remotely separated

regionally circulation features, which controls respectively droughts and floods over the US and East Asia, may be linked via recurring global modes which are underpinned by jetstream dynamics, and tropical heating in the Asian monsoon regions. Arguably, these global modes maybe important in pre-conditioning the large scale circulation to facilitate regional scale land-atmosphere interactions, leading to the occurrence of major droughts and floods over North America and East Asia.

Acknowledgment

The authors will like to thank Dr. K. M. Kim for plotting some of the color figures in the manuscript. Also acknowledged are suggestions and discussions by participants of the US Japan Monsoon System Workshop held at GSFC/Goddard Space Flight Center where this paper was first presented. This work is partially supported by, the NASA Earth Science Enterprise, Global Modeling and Analysis Program and the TRMM Program.

Table 1 Number of times when the reconstructed rainfall from Mode-1 and/or Mode-2 exceed the 95% and 99% confidence level, when compared to the observed rainfall from 1955-1998 (44 years).

	Before 1977		After 1977	
	> 95%	>99%	> 95%	> 99%
Mode –1 alone	2	1	6	3
Mode –2 alone	2	0	2	0
Mode 1 + 2	8	5	15	10

Figure Captions

Figure 1. Observed seasonal (JJA) precipitation total and seasonal mean circulation anomalies: a) rainfall over the US continent, b) 200 hPa velocity potential and divergent wind and c) 500 hPa geopotential and 850 hPa winds for 1993 (left panels) and 1998 (right panels).

Figure 2. One-point correlation of JJA mean rainfall anomaly over US Midwest region (shown in outlined box) with a) 500 hPa height and b) SST. The contour interval is 0.1. Correlation values larger than 0.3 (> 95% confidence level) are dark (positive) and light (negative) shaded.

Figure 3. Spatial distribution and principal components of JJA US rainfall anomalies for a) EOF1 and b) EOF2. The contours in the spatial pattern have been scaled by the standard deviation of the rainfall variability with contour interval of 10 mm, and with the positive values shaded. The principal components are non-dimensional.

Figure 4. Spatial patterns of SVD1 between JJA US rainfall and 500 hPa geopotential height for a) US rainfall, b) 500 hPa geopotential height, and c) corresponding principal components (non-dimensional). The contour interval is 10 mm in (a), and that is 2 gpm in (b). Positive values are shaded.

Figure 5. Same as in Fig. 4, except for SVD2.

Figure 6. Same as in Fig. 4, except for SVD1 between US rainfall and SST. The contour interval is 10 mm in (a) and 0.1°C in (b)

Figure 7 Same as in Fig. 4 except for SVD2 between US rainfall and global SST.

Figure 8. Global regression of a) 500 hPa height and 850 hPa wind, and b) and 200 hPa velocity potential and divergent wind against the principal components of Mode-1; c) and d) are the same as a) and b) respectively, but for Mode-2.

Figure 9. Mode-by-Mode reconstruction of observed JJA US rainfall anomalies for 1993, based on SVDs between US rainfall and global SST. The contour interval is 20 mm. Values larger than 80 mm are dark (positive) and light (negative) shaded.

Figure 10. Same as in Fig. 9, except for 1988 JJA.

Figure 11. Cumulative anomaly correlation between reconstructed and observed rainfall anomalies using the first five SVD modes based on a) PC for rainfall, and b) PC for SST. Contributions from Mode-1, Mode-2 and Mode 3-5 (combined) are indicated by heavy, medium and light shaded bars, respectively.

Figure 12. Spatial distribution of SVD2 (upper panels) and of SVD3 (lower panels) between rainfall over China and global SST. The contour interval for rainfall (left panels) is 20 mm, and that for SST (right panels) is 0.1°C. Positive and negative values are dark and light shaded, respectively.

Figure 13. Linear regression of 500 hPa geopotential height and 850 hPa wind against the principal components of (a) SVD2 and (b) SVD3 between China rainfall and global SST.

Figure 14. Linear regression of 850 hPa wind and rainfall over China and the US against a) the East Asian monsoon index and b) the Western North Pacific Monsoon index. See text for definition of indices.

References

Bosilovich, M, G., and W. Y. Sun, 1999: Numerical simulation of the 1993 midwestern flood: land-atmosphere interactions. *J. Climate,* **12**, 1490- 1505.

Bretherton, C. S., M. Widmann, V. P. Dymnikov,J. M. Wallace and I. Blade, 1999: The effective number of spatial degrees of freedom of a time varying field. *J. Climate*, **12**, 1990-2009.

Chen, P., and M. Newman, 1998: Rossby wave propagation and the rapid development of upper level anomalous anticyclones during the 1988 U. S. Drought. *J. Climate*, **11**, 2491-2503.

Chen, T. C., 1993: Interannual variation of summertime stationary eddies. *J. Climate*, **6**, 2263-2277.

Cherry, S, 1997: Some comments on singular value decomposition analysis. *J. Climate*, **10,** 1759-1761.

Graham, N.E., 1994: Decadal scale climate variability in the tropical and North Pacific during the 1970s and 1980s: observation and model results. *Clim. Dyn.*, **10**. 135-162.

Higgins, R. W., A. Leetmaa, Y. Xue and A. Barnston, 2000: Dominant factors influencing the seasonal predictability of United States precipitation and surface air temperature. *J. Climate*. (in press).

Higgins, R. W., Y. Chen and A.V. Douglas, 1999: Interannual variability of the North American warm season precipitation regime. *J. Climate*, **12**, 653-680.

Huang, R., 1985: Numerical simulation of the three-dimensional teleconnection in the summer circulation over the Northern Hemisphere. *Adv. Atmos. Sci.*, **2**, 81-92.

Kalnay, E., M. Kanamitsu, R. Kistler, W. Collins, D. Deaven, L. Gandin, M. Iredell, S. Saha, G. White, J. Woollen, Y. Zhu, M. Chelliah, W. Ebisuzaki, W. Higgins, J.

Janowiak, K. C. Mo, C. Ropelewski, J. Wang, A. Leetmaa, R. Reynolds, R. Jenne and D. Joseph, 1996: The NCEP/NCAR 40-year reanalysis Project. *Bull. Am. Meteor. Soc.*, **77**, 437-471.

Krishnamurthy, V., and B. N. Goswami, 2000: Indian Monsoon-ENSO relationship on interdecadal timescale. *J. Climate*, 13, 579-595.

Kumar, K. Krishna, Balaji Rajagopalan, Mark A. Cane, 1999: On the weakening relationship between the Indian Monsoon and ENSO. Science, 284, 2156-2159.

Lau, K. M, 1992: East Asian summer monsoon variability and climate teleconnection. *J. Meteor. Soc. Japan*, **70**, 211-242.

Lau, K. M. and H. T. Wu,, 2001: Intrinsic modes of coupled rainfall/SST variability for the Asian summer monsoon: a re-assessment of monsoon-ENSO relationship. J. Climate (in press).

Lau, K. M. and H. Weng, 2001: Coherent modes of global SST and summer rainfall over China: an assessment of the regional impacts of the 1997-98 El Nino. *J. Climate* (in press).

Lau, K. M. and H. Weng, 2000: Remote forcing of US summertime droughts and floods by the Asian monsoon? *GEWEX News*, **10**, May issue, 5-6.

Lau, K. M. and H. Weng, 1999: Interannual, decadal-interdecadal and global warming signals in sea surface temperature during 1955-97. J. Climate, 12, 1257-1267.

Lau, K. M. and H. T. Wu, 1999: An Assessment of the impact of the 1997-98 El Niño on the Asian-Australian monsoon. *Geophys. Res. Lett.*, **26**, 1747-1750.

Lau, K. M., and L. Peng, 1992: Dynamics of atmospheric teleconnections during the Northern Hemisphere summer. *J. Climate.*, **5**, 140-158.

Lau, K. M., K. M. Kim, and S. Yang, 2000: Dynamical and Boundary Forcing Characteristics of regional components of the Asian summer monsoon. *J. Climate,* **13,** 2461-2482.

Lau, N. C., and M. J. Nath, 1996: The role of "atmospheric bridge" in linking tropical Pacific ENSO events to extratropical SST anomalies. *J. Climate*, **9**, 2036-2057.

Li, Chongyin and L. Zhang, 1999: Summer monsoon activities in South China Sea and its impacts. *Chinese J. Atmos. Sci.,* **23**, 111-121.

Liu, A. Z., M. Ting and H. Wang, 1998: Maintenance of circulation anomalies during the 1988 drought and the 1993 floods over the United States. *J. Atmos. Sci.*, **55**, 2810-2832.

Livezey, R., and T. M. Smith, 1998: Covariability of aspects of North American climate with global sea surface temperatures on interannual to interdecadal timescales. *J. Climate,* **12**, 289-302.

Mo, K. C. , and E. Kalnay, 1991: Impact of sea surface temperature anomalies on the skill of monthly forecasts. *Mon. Wea. Rev.*, **119,** 2771-2793.

Mo, K. C. ,J. R. Zimmerman, E. Kalnay and M. Kanamitsu, 1991: A GCM study of the 1988 United States drought. *Mon. Wea. Rev.*, **119**, 1512-1532.

Mo, K. C., 2000: Intraseasonal modulation of summer precipitation over North America. *Mon. Wea. Rev.*, **128**, 1490-1505.

Mo, K. C., J. N. Paegle, and R. W. Higgins, 1997: Atmospheric processes associated with summer floods and droughts in the central United States. *J. Climate*, **10**, 3028-3046.

Newman, M, and P. D. Sardesmukh, 1995: A caveat concerning singular value decomposition. *J. Climate*, **8**, 352-360.

Nitta, T., 1987: Convective activities in the tropical western Pacific and their impact on the northern hemisphere summer circulation. *J. Meteor. Soc. Japan*, **41**, 373-390.

Palmer, T. N., and C. Brankovic 1989: The 1988 U.S. drought linked to anomalous sea-surface temperature. *Nature*, **338**, 554-557.

Sardesmukh , P. and B. Hoskins, 1988: The generation of global rotational flow by steady idealized tropical divergence, *J. Atmos. Sci.* **45**, 1228-1251.

Ting, M. and H. Wang, 1997: Summertime U. S. precipitation variability and its relation to Pacific sea surface temperature. *J. Climate*, **10,** 1853-1873.

Trenberth, K., and C. J. Guillemot, 1995: Physical processes involved in the 1988 drought and 1993 floods in North America. *J. Climate*, **9,** 1288-1298.

Trenberth, K. E., and G. W. Branstator, 1992: Issues in establishing causes of the 1988 drought over North America. *J. Climate*, **5**, 159-172.

Trenberth, K. E., G. W. Branstator and P. A. Arkin, 1988: Origins of the 1988 North American drought, *Science*, **242**, 1640-1645.

Wallace J. M., C. Smith and C. S. Bretherton, 1991: Singular value decomposition of wintertime sea surface temperature and 500 mb height anomalies. *J. Climate*, **5**. 561-576.

Wang, B., and Z. Fan, 1999: Choice of South Asian summer monsoon indices. *Bull. Am. Meteor. Soc.*, **80**, 629-638.

Wang, B., R. Wu and K. M. Lau, 2001: Contrasting interannual variations between the Indian and the western North Pacific summer monsoon. *J. Climate* (submitted).

Weng, H., K. M. Lau and Y.-K. Xue, 1998: Long-term variability of summer rainfall over China and its possible link to global sea surface temperature variability. *J. Meteor. Soc. Japan*, **77**, 845-857.

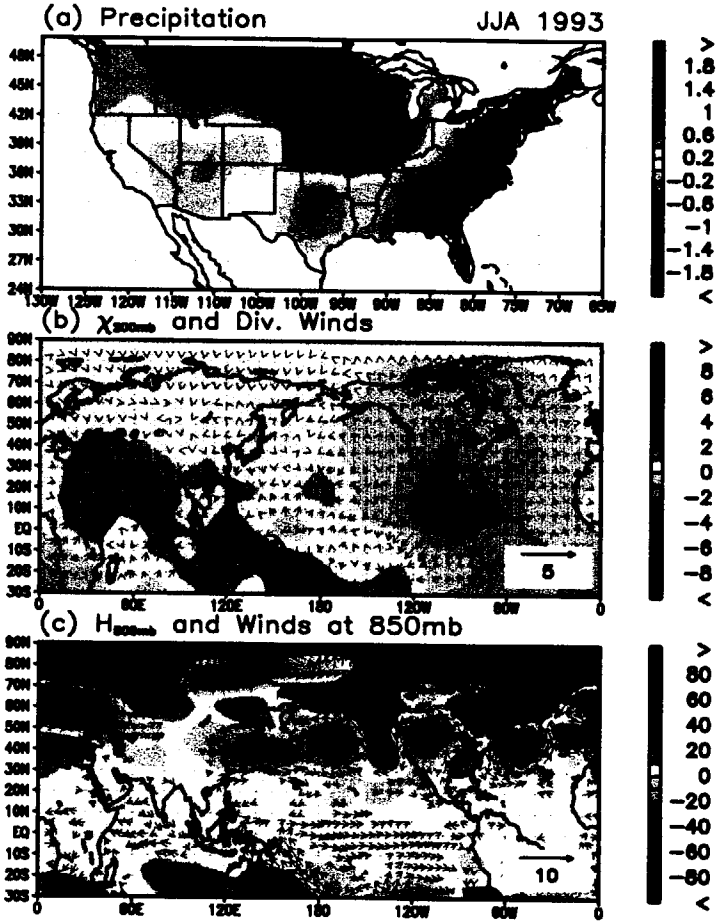
(a) Precipitation
JJA 1993
(b) χ_{200mb} and Div. Winds
(c) H_{500mb} and Winds at 850mb

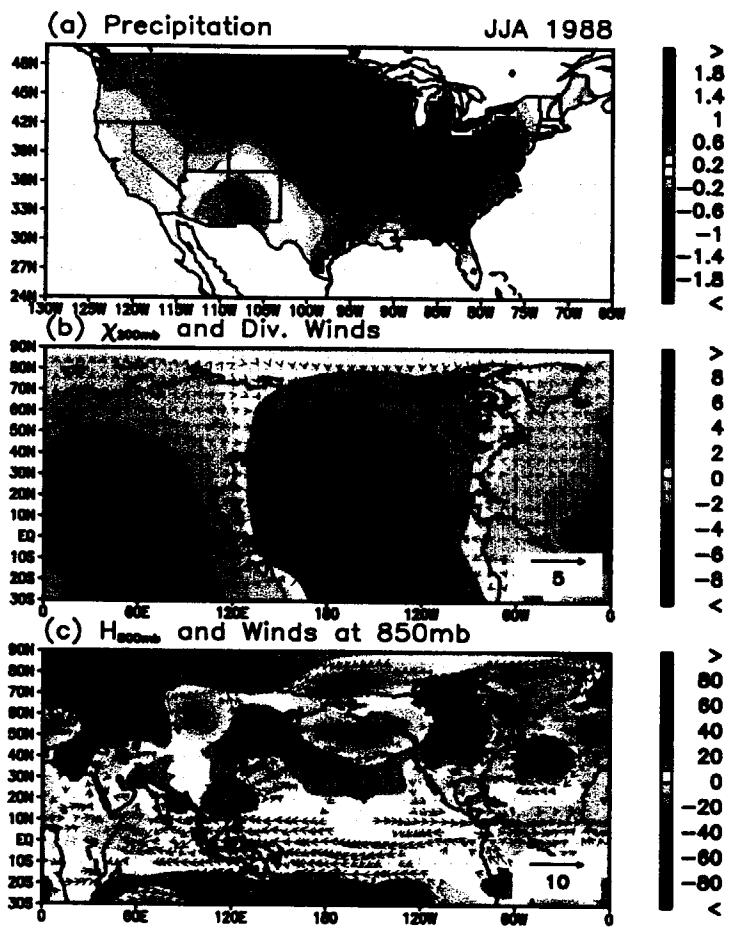
(a) Precipitation
JJA 1988
(b) χ_{200mb} and Div. Winds
(c) H_{500mb} and Winds at 850mb

Fig 1

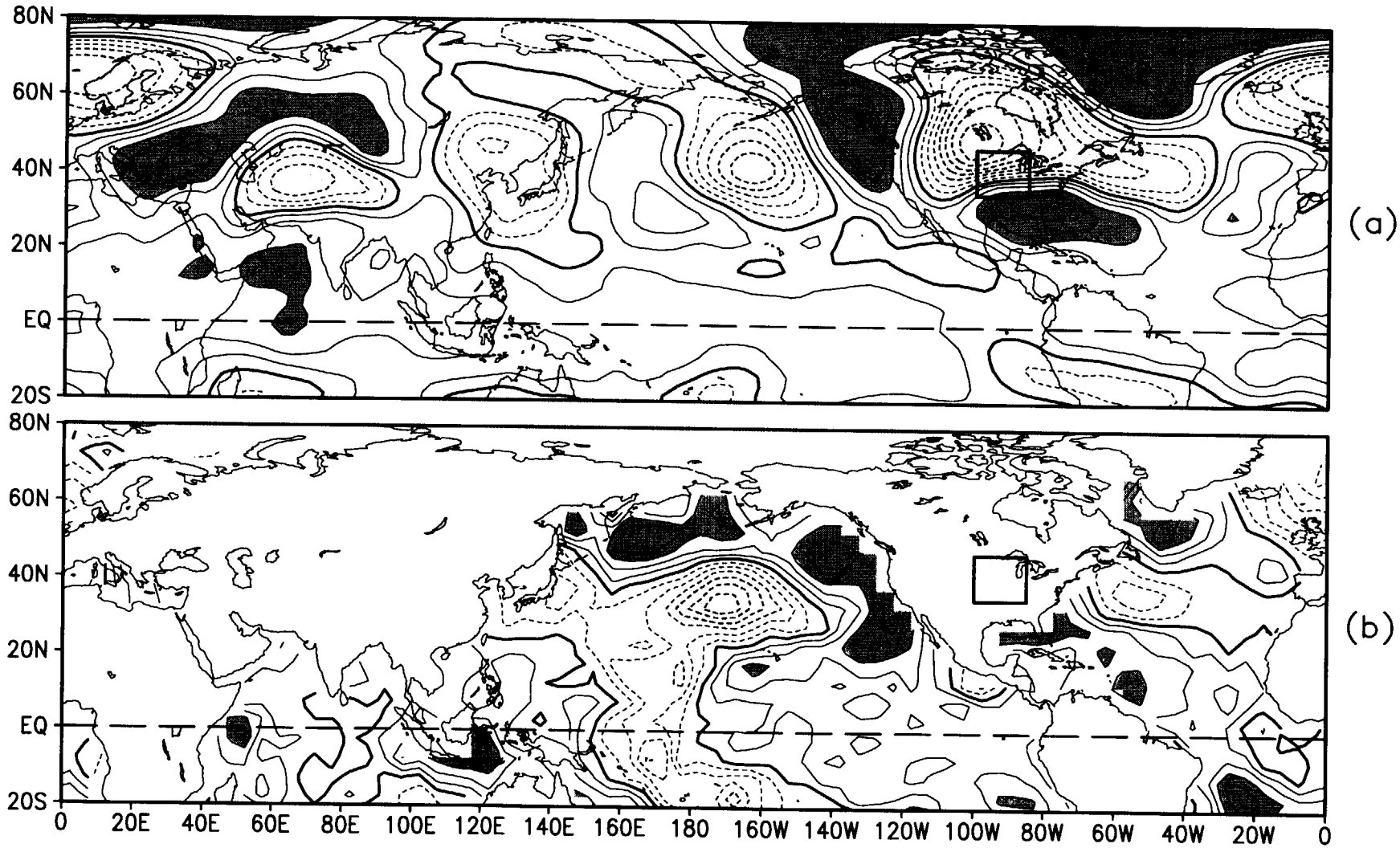
80N
60N
40N
20N
EQ
20S
(a)
80N
60N
40N
20N
EQ
20S
(b)
0
20E
40E
60E
80E
100E
120E
140E
160E
180
160W
140W
120W
100W
80W
60W
40W
20W
0

Fig 2

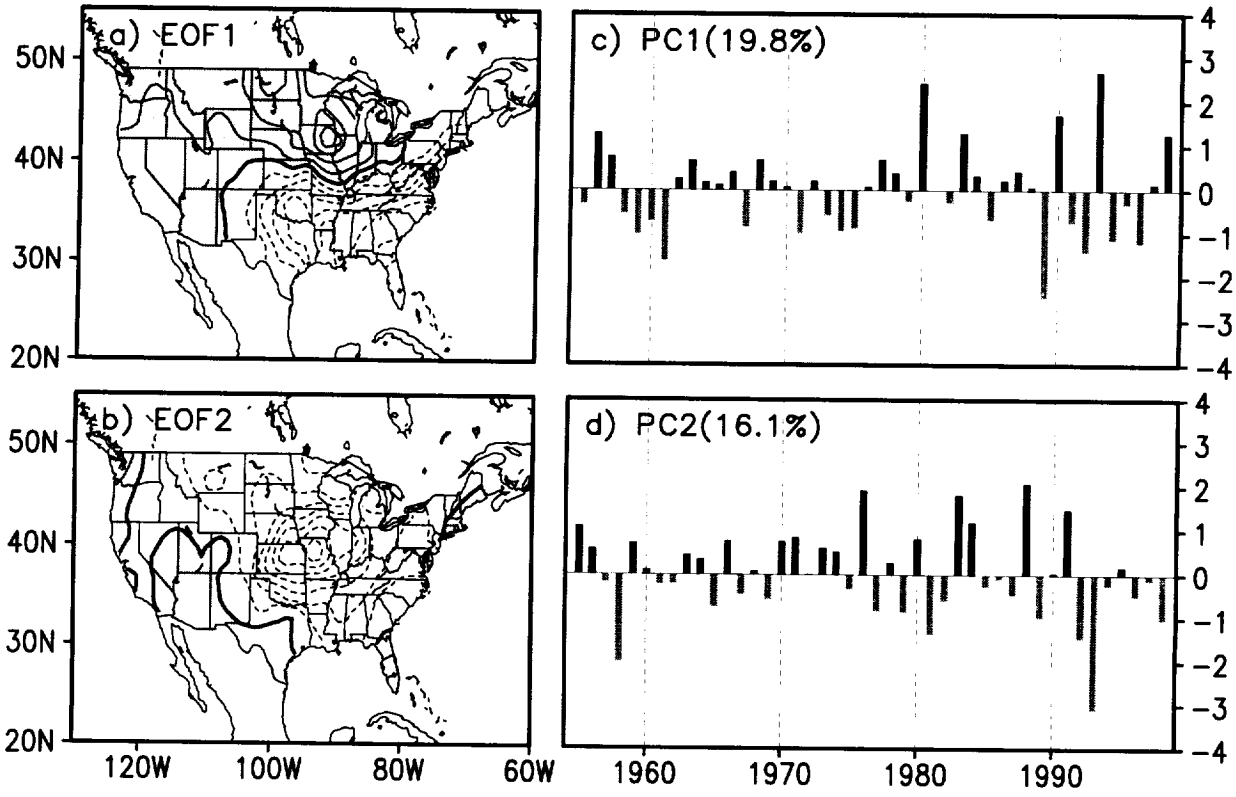
a) EOF1
b) EOF2
c) PC1(19.8%)
d) PC2(16.1%)
50N
40N
30N
20N
120W
100W
80W
60W
1960
1970
1980
1990
4
3
2
1
0
−1
−2
−3
−4

Fig 3

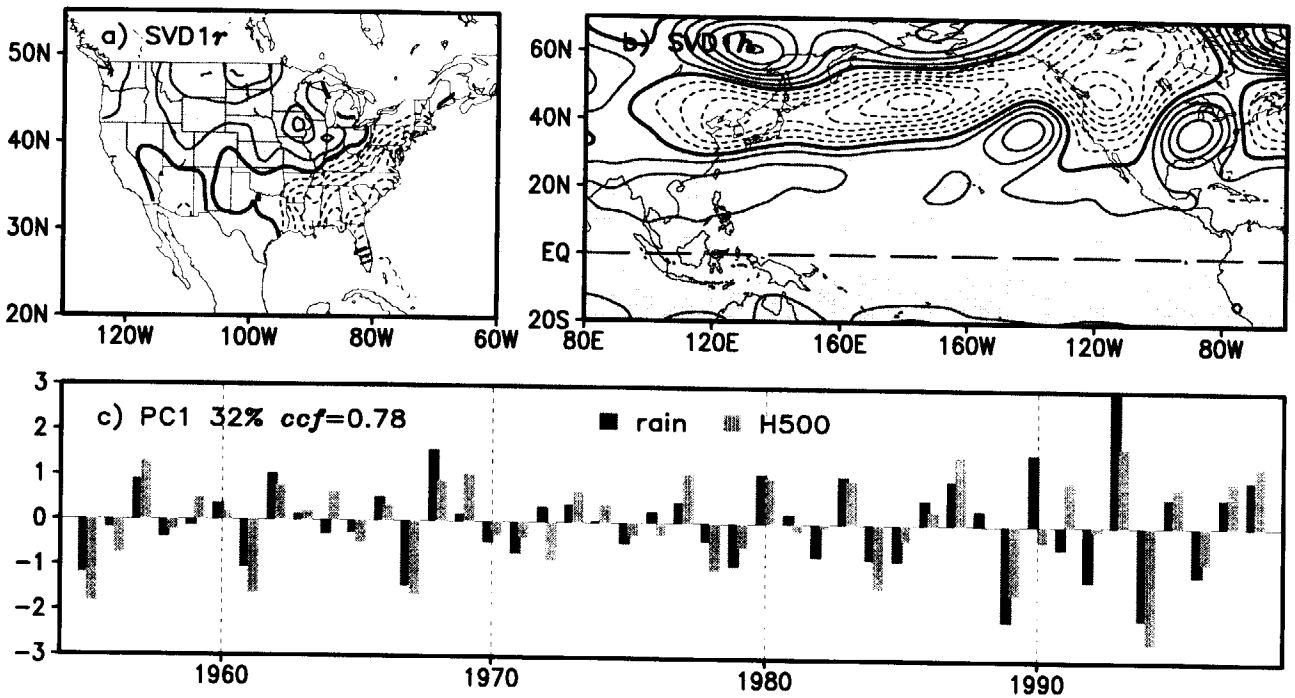
a) SVD1r
50N
40N
30N
20N
120W
100W
80W
60W
b) SVD1h
60N
40N
20N
EQ
20S
80E
120E
160E
160W
120W
80W
c) PC1 32% ccf=0.78
rain
H500
3
2
1
0
−1
−2
−3
1960
1970
1980
1990

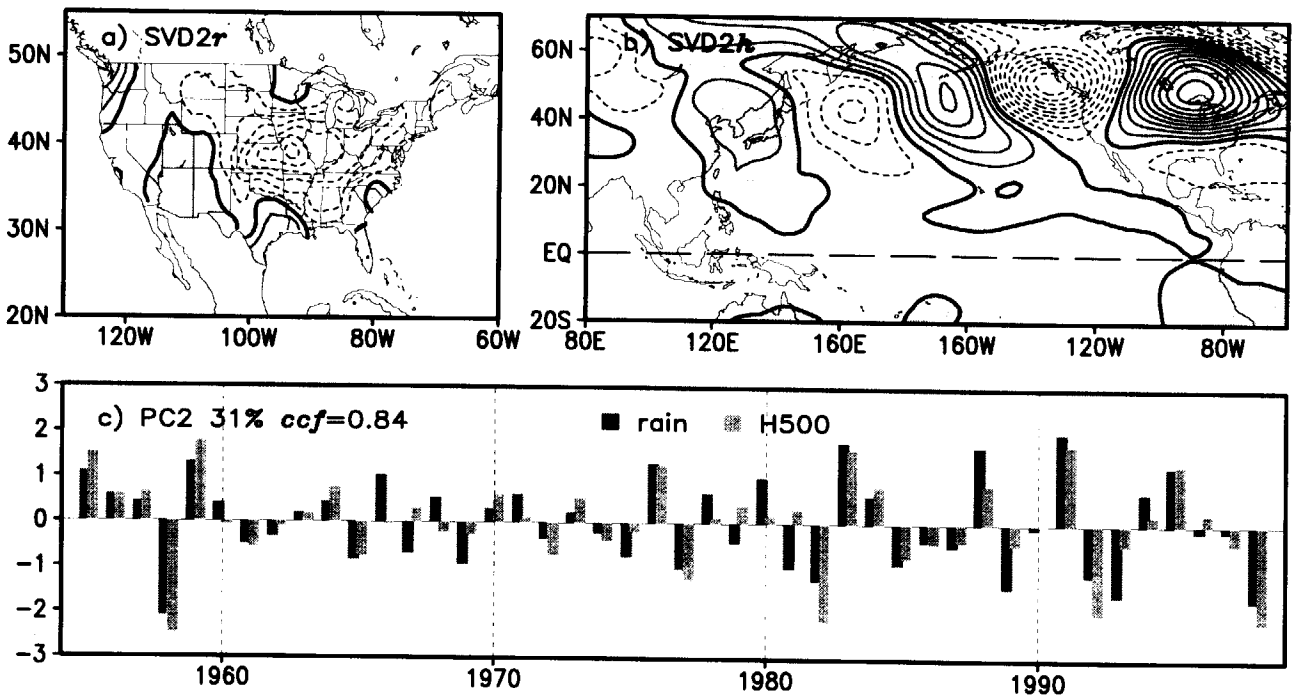
a) SVD2r
50N
40N
30N
20N
120W
100W
80W
60W
b) SVD2h
60N
40N
20N
EQ
20S
80E
120E
160E
160W
120W
80W
c) PC2 31% ccf=0.84
rain
H500
3
2
1
0
−1
−2
−3
1960
1970
1980
1990

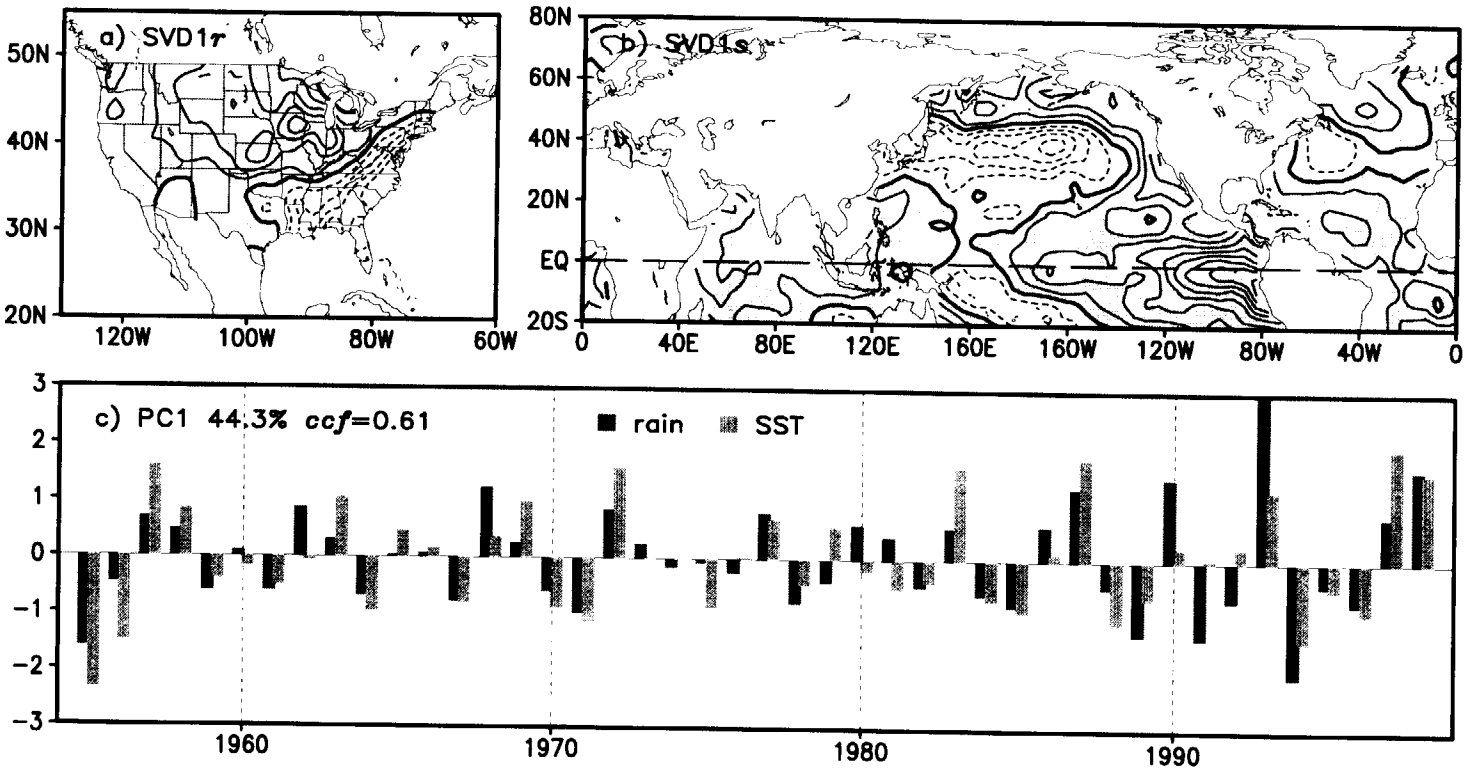
a) SVD1r
50N
40N
30N
20N
120W
100W
80W
60W
b) SVD1s
80N
60N
40N
20N
EQ
20S
0
40E
80E
120E
160E
160W
120W
80W
40W
0
c) PC1 44.3% ccf=0.61
rain
SST
3
2
1
0
−1
−2
−3
1960
1970
1980
1990

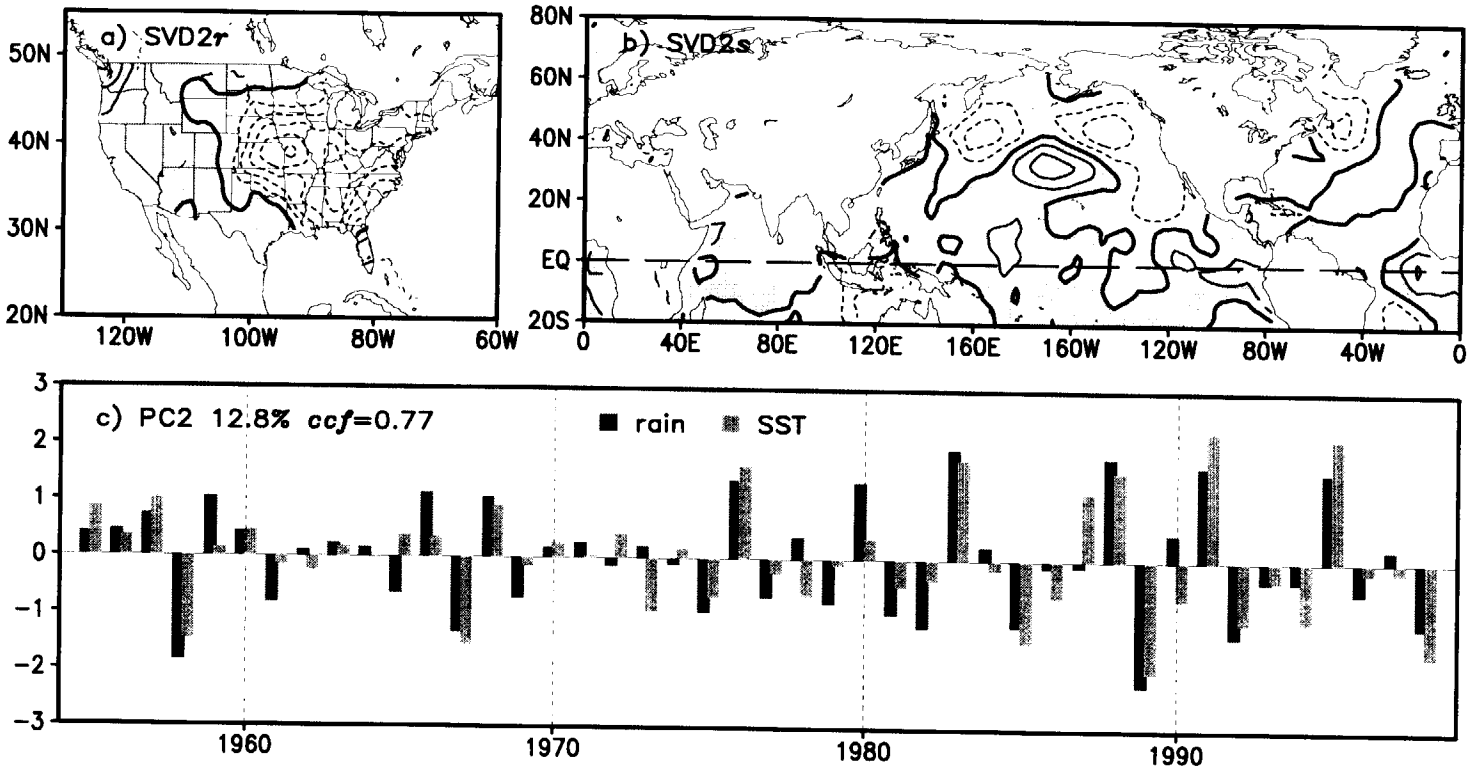
a) SVD2r
50N
40N
30N
20N
120W
100W
80W
60W
b) SVD2s
80N
60N
40N
20N
EQ
20S
0
40E
80E
120E
160E
160W
120W
80W
40W
0
c) PC2 12.8% ccf=0.77
rain
SST
3
2
1
0
−1
−2
−3
1960
1970
1980
1990

Fig. 7

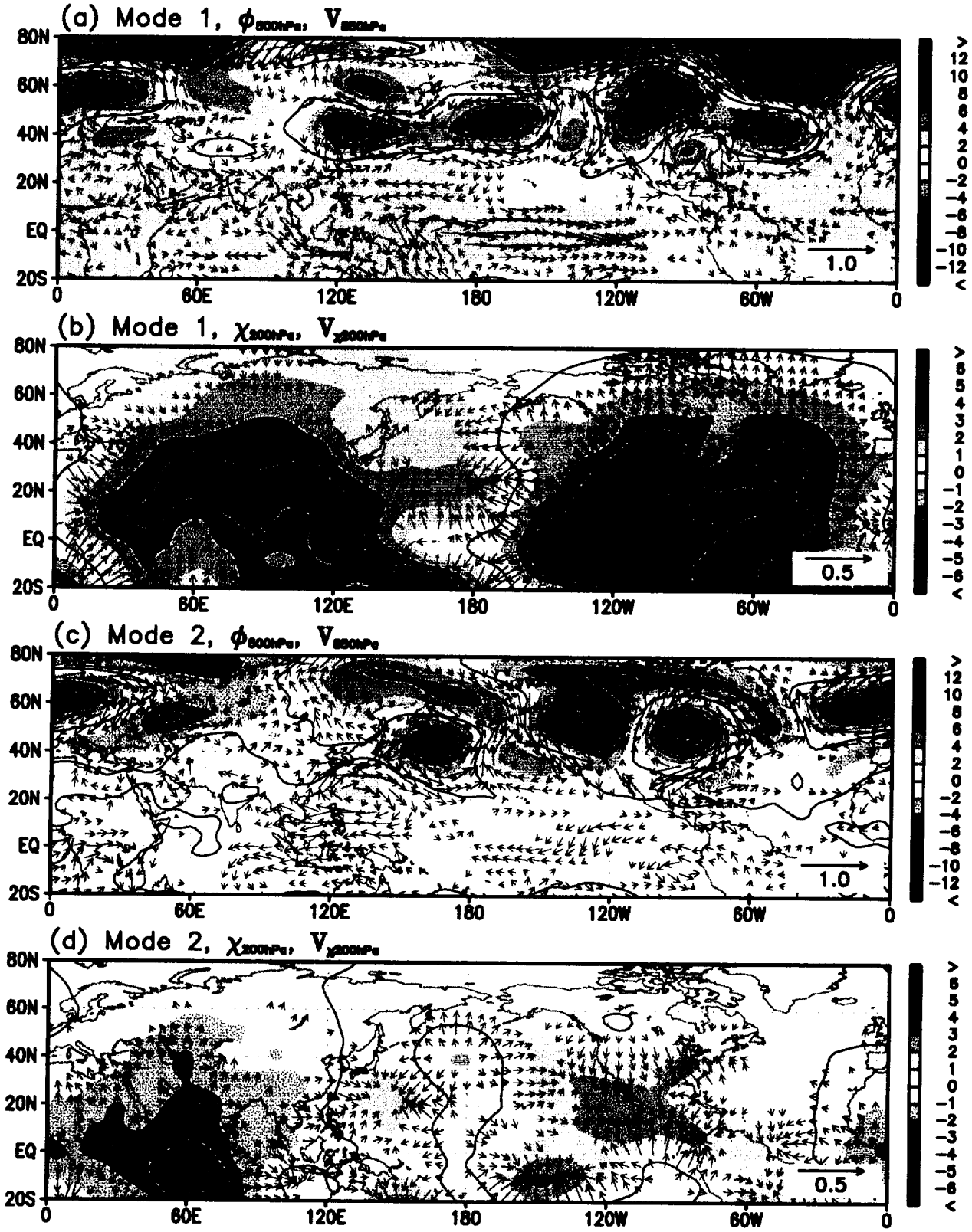
(a) Mode 1, ϕ_{200hPa}, V_{850hPa}
80N
60N
40N
20N
EQ
20S
0
60E
120E
180
120W
60W
0
1.0
> 12 10 8 6 4 2 0 -2 -4 -6 -8 -10 -12 <
(b) Mode 1, χ_{200hPa}, $V_{\chi 200hPa}$
0.5
> 6 5 4 3 2 1 0 -1 -2 -3 -4 -5 -6 <
(c) Mode 2, ϕ_{200hPa}, V_{850hPa}
1.0
> 12 10 8 6 4 2 0 -2 -4 -6 -8 -10 -12 <
(d) Mode 2, χ_{200hPa}, $V_{\chi 200hPa}$
0.5
> 6 5 4 3 2 1 0 -1 -2 -3 -4 -5 -6 <

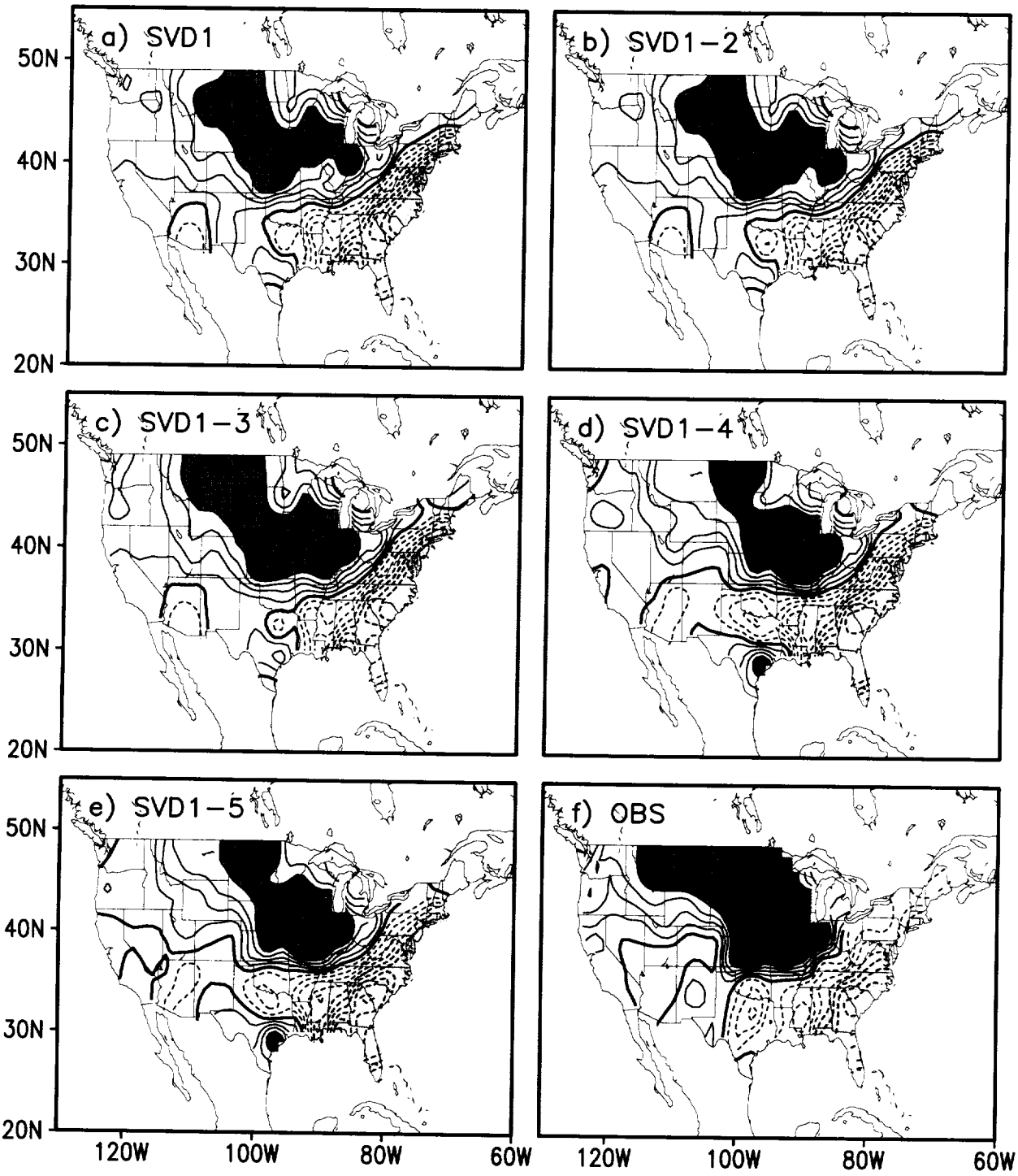
1993 summer
a) SVD1
b) SVD1−2
c) SVD1−3
d) SVD1−4
e) SVD1−5
f) OBS
50N
40N
30N
20N
120W
100W
80W
60W

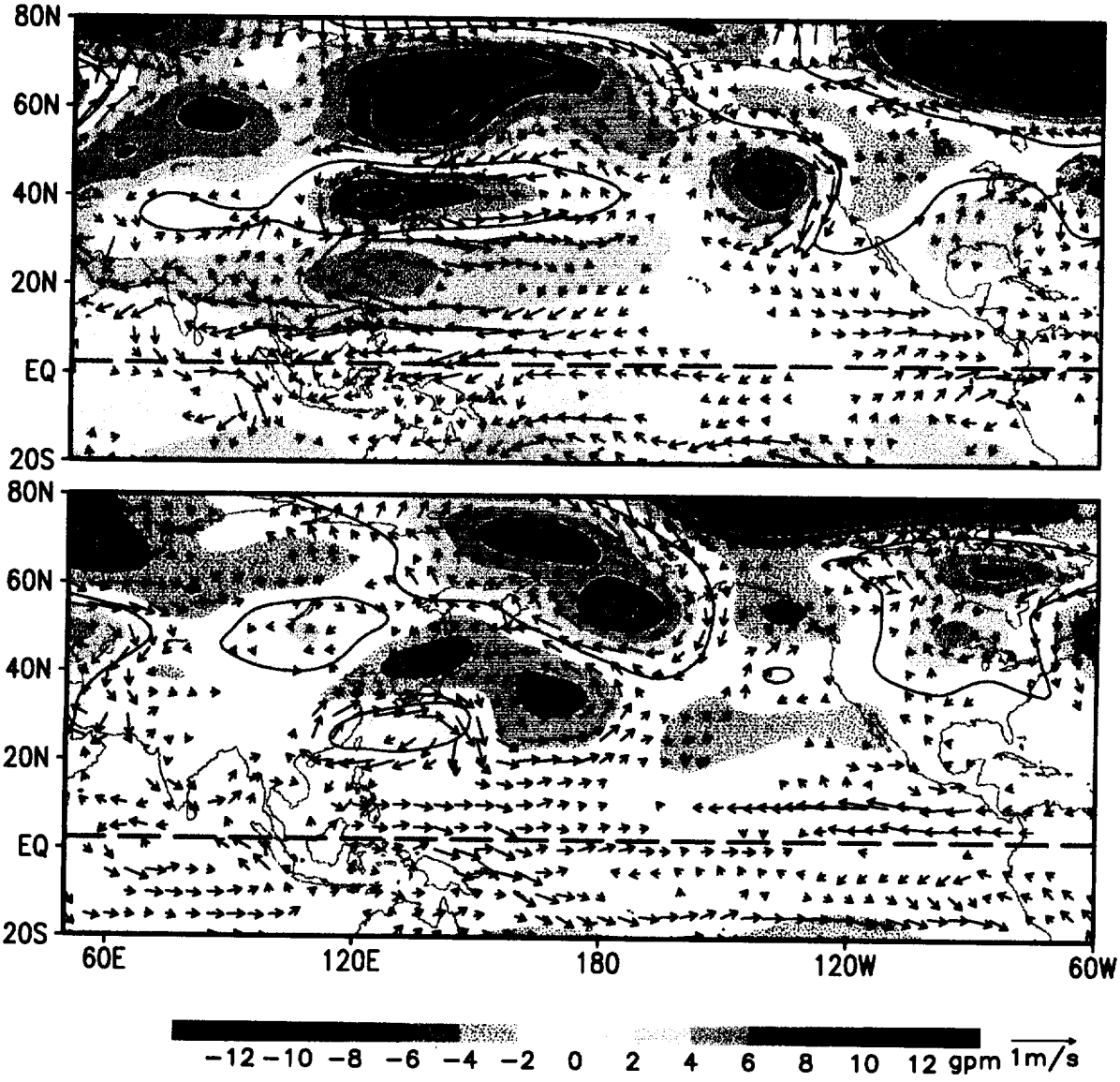
80N
60N
40N
20N
EQ
20S
80N
60N
40N
20N
EQ
20S
60E
120E
180
120W
60W
−12 −10 −8 −6 −4 −2 0 2 4 6 8 10 12 gpm
1m/s

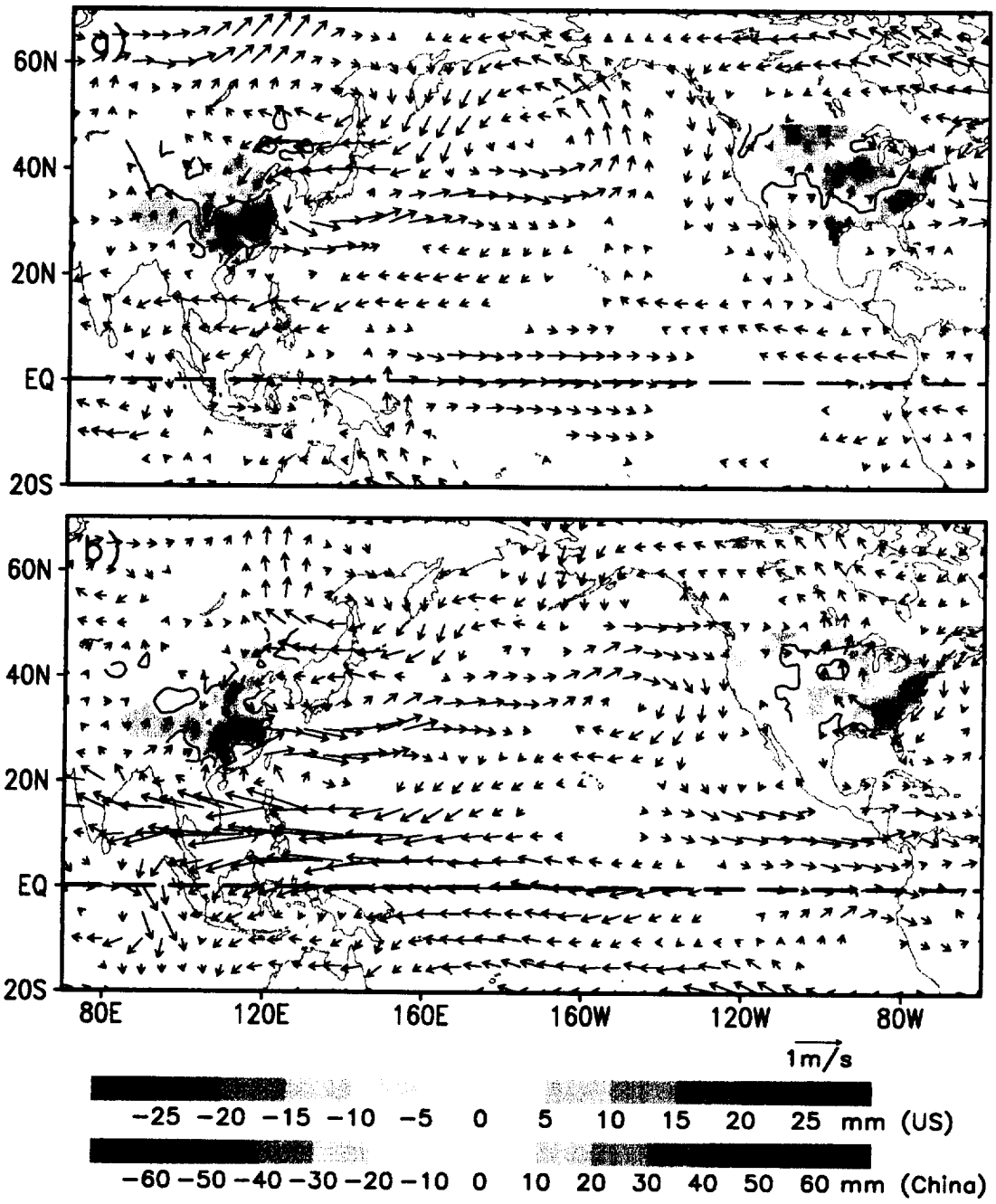
a)
b)
60N
40N
20N
EQ
20S
80E
120E
160E
160W
120W
80W
1m/s
−25 −20 −15 −10 −5 0 5 10 15 20 25 mm (US)
−60 −50 −40 −30 −20 −10 0 10 20 30 40 50 60 mm (China)